Semicond. Sci. Technol. **26** (2011) 125006 (6pp) doi:10.1088/0268-1242/26/12/125006

Electrical and photoelectrical properties of photosensitive heterojunctions n-TiO_2/p-CdTe

V V Brus[1,3], M I Ilashchuk[2], Z D Kovalyuk[1], P D Maryanchuk[2] and K S Ulyanytsky[2]

[1] Frantsevich Institute for Problems of Materials Science, NAS of Ukraine, Chernivtsi Branch, 58001 Chernivtsi, Ukraine,
[2] Yuriy Fedkovych Chernivtsi National University, 58012 Chernivtsi, Ukraine

E-mail: victorbrus@mail.ru and p.maryanchuk@chnu.edu.ua

Received 25 July 2011, in final form 30 September 2011
Published 3 November 2011
Online at stacks.iop.org/SST/26/125006

Abstract
Photosensitive heterojunctions n-TiO_2/p-CdTe were fabricated by dc reactive magnetron deposition of TiO_2 thin films with n-type conductivity onto freshly cleaved p-CdTe single-crystal substrates (1 1 0). Their electrical properties were investigated and the dominating current mechanisms were analyzed at forward and reverse biases in the scope of the tunnel-recombination and emission-recombination models. The obtained surface-barrier structures n-TiO_2/p-CdTe possessed the following photoelectrical parameters under 100 mW cm^{-2} illumination: the open-circuit voltage $V_{oc} = 0.69$ V, the short-circuit current $I_{sc} = 6$ mA cm^{-2} and the fill factor FF = 0.42.

1. Introduction

Currently, many different prospective materials and structures for application in highly efficient solar cells present objects of great scientific interest because the application of heterojunctions in photoelectric convertors enhances their functional capabilities and operational characteristics compared with photoelectrical devices based on homojunctions [1, 2].

The promising thin film heterojunctions CdS/CdTe have been under intensive investigation over the last few years [3–5]. This process is caused by the optimal physical properties of CdTe for highly efficient conversion of solar energy. The highest efficiency of the thin film CdS/CdTe solar cells is reported to be 16.5% [6], which is significantly less than the theoretical limit of their efficiency ~30%. There are a lot of experimental and theoretical works that deal with the dependence of the efficiency of CdS/CdTe solar cells on factors that are mainly determined by the properties of the base material (CdTe), in particular, the width of the space charge region, the lifetime of minority charge carriers, their diffusion length, the width of the CdTe absorbing layer and the velocity of surface recombination, etc [4, 7–10]. The reason is that the photoelectrical conversion takes place only in the CdTe film. However, at the same time, the frontal layer CdS intensively absorbs light at the wavelength $\lambda < 520$ nm, thereby reducing the photocurrent [4, 10]. The losses caused by the light absorption in the 'window' layer of CdS/CdTe solar cells can be reduced by using a material with a wider band gap instead of CdS.

Titanium dioxide (TiO_2), one of the best prospective transparent conductive oxides, is widely used in different semiconductor devices due to its high transparency for visible light, large value of the refractive index, controllable specific resistance, good adhesion and high chemical resistance [11]. Also, TiO_2 is environment friendly.

The value of the band gap energy of TiO_2 varies from 3.15 to 3.5 eV depending on the crystalline structure and deposition technology [11–13], that is, about 1 eV larger than that of CdS. This characteristic of TiO_2 allows broadening of the spectral region of the photosensitivity of heterojunctions based on CdTe toward the short wavelengths.

Therefore, according to the above-mentioned fact, n-TiO_2/p-CdTe heterojunctions are considered to be suitable for highly efficient photoelectric conversion. This has been

[3] Author to whom any correspondence should be addressed.

confirmed in a number of experimental works, where the solar cells based on a TiO_2/CdTe heterojunction were fabricated [14, 15]. However, to the best of our knowledge, the mechanisms of the current transport through the n-TiO_2/p-CdTe heterojunctions as well as their electrical properties have not been yet investigated in detail. It is obvious that the absence of a clear understanding of the electrical processes that take place at the TiO_2/CdTe interface strongly influences the improvement of the existing solar cells and design of the new solar cells based on the n-TiO_2/p-CdTe heterojunctions.

This paper reports the results of an investigation on the electrical and photoelectrical properties of the n-TiO_2/p-CdTe heterojunctions, prepared by means of the deposition of TiO_2 thin films onto the freshly cleaved p-CdTe single-crystal substrates, and establishing the dominating current mechanisms through the heterojunctions at the forward and reverse biases.

2. Experimental methods

2.1. The n-TiO_2/p-CdTe heterojuction fabrication

The CdTe single crystals with p-type conductivity were grown by the Bridgman method at low cadmium vapor pressure ($P_{Cd} = 0.02$ bar). The values of specific electrical conductance and majority carriers concentration at 295 K for these crystals were measured to be $\sigma = 8.9 \times 10^{-2}$ Ω^{-1} cm^{-1} and p $= 7.2 \times 10^{15}$ cm^{-3}, respectively. The energy location of the Fermi level according to the top of the valance band of CdTe ($E_F - E_v = 0.105$ eV) was determined by employing the following equation for the equilibrium hole concentration in a non-degenerate semiconductor: $p = 2(2\pi m_p kT/h^2)^{3/2} \exp(-(E_F - E_v))/kT$.

The TiO_2 thin films were deposited onto the freshly cleaved p-CdTe single-crystal substrates (1 1 0) with typical dimensions 5 × 4 × 1 mm in a universal coating system Laybold–Heraeus L560 by dc reactive magnetron sputtering of a titanium target in atmosphere of the argon and oxygen mixture.

The titanium target, a cylinder of 100 mm diameter and 5 mm thickness, was mounted on the magnetron table under water cooling 7 cm from the substrates.

The CdTe substrates were mounted over the magnetron on a rotating substrate holder for providing uniform thickness of the films. Before the deposition process started, the vacuum chamber was pumped down to a residual pressure of 5×10^{-5} mbar.

Pure argon and oxygen from two separate sources were mixed in the desirable ratio.

A short-term sputter cleaning of the target and substrates by Ar ions was applied to eliminate the surface contaminants.

During the deposition process, the partial pressures of argon and oxygen were equal to 7×10^{-3} and 2×10^{-4} mbar, respectively. The magnetron power was 350 W. The substrate temperature was 573 K. The deposition process lasted for 20 min.

The TiO_2 thin films were also simultaneously deposited onto glass ceramic substrates for determining the electrical parameters of the thin film. The obtained TiO_2 thin film possessed n-type of conductivity. The measured values of specific electrical conductance and majority carriers concentration at 295 K for the TiO_2 thin films were $\sigma = 0.71$ Ω^{-1} cm^{-1} and $n = 4.8 \times 10^{17}$ cm^{-3}, respectively.

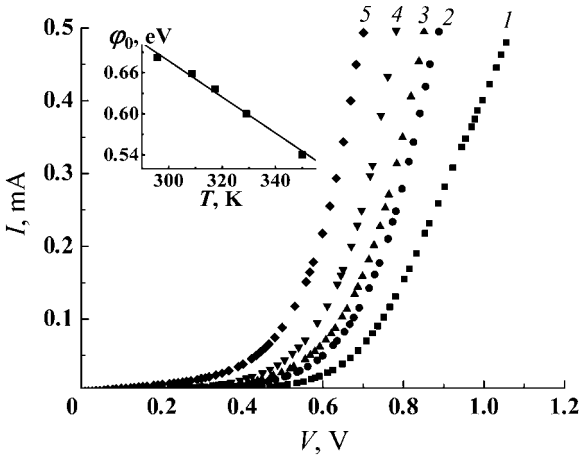

Figure 1. The *I–V* characteristics of the n-TiO_2/p-CdTe heterojunctions: 1—295 K, 2—309 K, 3—318 K, 4—329 K, 5—350 K. The inset shows the temperature dependence of the height of the potential barrier.

2.2. The ohmic contact fabrication

The frontal point contacts to the heterojunctions were fabricated by thermal evaporation of indium onto the TiO_2 thin films at the substrate temperature of 373 K [16].

Before the back contacts were prepared, the back surface of the heterojunctions (p-CdTe) was exposed to a monopulse of a powerful ruby laser with the wavelength $\lambda = 0.694$ μm and pulse duration $\tau = 1.2$ ms in order to create a p$^+$ layer due to additionally generated cadmium vacancies on the back surface. The Au and Cu layers were successively deposited onto the laser-treated back surface by means of reduction from aqueous solutions of gold chloride and copper vitriol, respectively.

The electrophysical parameters of the components of the heterojunctions were measured by means of the conventional two-probe method in the direct current mode.

The dark and light current–voltage (*I–V*) characteristics of the n-TiO_2/p-CdTe heterojunctions were measured by a SOLARTRON SI 1286, SI 1255 complex at different temperatures.

The spectral distribution of the external quantum efficiency of the n-TiO_2/p-CdTe heterojunctions was measured by a conventional spectrophotometer within the range of wavelength from 350 to 900 nm.

3. Results and their discussion

3.1. Electrical properties

Figure 1 shows the forward branches of the *I–V* characteristics of the anisotype heterojunctions n-TiO_2/p-CdTe, measured at different temperatures.

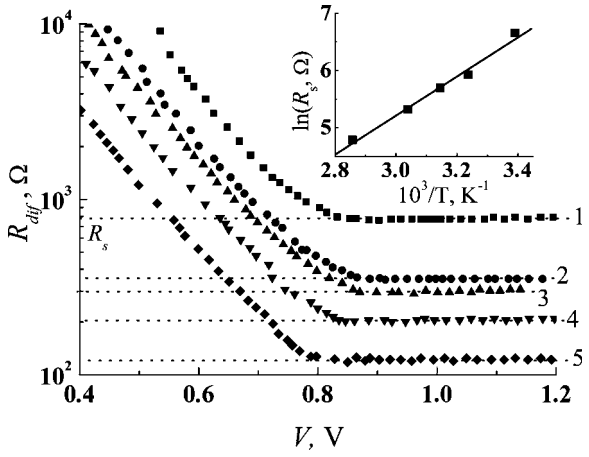

Figure 2. The dependence of the deferential resistance of the heterojunctions on voltage under forward bias: 1—295 K, 2—309 K, 3—318 K, 4—329 K, 5—350 K. The inset shows the temperature dependence of the serial resistance.

The height of the potential barrier was determined by the extrapolation of the linear segments of the *I–V* characteristics at different temperatures toward the interception with the voltage axis (the inset of figure 1). The temperature dependence of the height of the potential barrier of the n-TiO_2/p-CdTe heterojunctions can be well described by the linear equation

$$\varphi_0(T) = \varphi_0(0) - \beta_\varphi \cdot T, \tag{1}$$

where $\beta_\varphi = 2.85 \times 10^{-3}$ eV K^{-1} is the temperature coefficient of the height of the potential barrier, and $\varphi_0(0) = 1.47$ eV is the value of the height of the potential barrier at zero temperature.

The value of the serial resistance of the heterojunction R_s can be found from the voltage dependence of their differential resistance R_{dif} at a forward bias (figure 2) [17]. It is seen that at the low voltages, the differential resistance decreases linearly in the semilogarithmic coordinates as the voltage increases. If the voltage elevates further, the $R_{dif}(V)$ curves become saturated. The value of the serial resistance of the heterojunctions R_s can be determined by the extrapolation of the saturated segments of the $R_{dif}(V)$ curves toward the interception with the axis of the differential resistance.

It should be noted that the determined value of the serial resistance R_s at 295 K is equal to 780 Ω, that is, three times larger than the resistance of the single-crystal CdTe substrate at the same temperature ($R_{CdTe} = 250$ Ω).

The value of the serial resistance R_s is proportional to the specific resistance ρ, which is given by the following equation in the case of a partially compensated semiconductor-like CdTe:

$$\rho = \frac{1}{q\mu_p p} = \frac{1}{q\mu_p N_v \frac{N_a - N_d}{2N_d} \exp\left(-\frac{E_A}{kT}\right)}, \tag{2}$$

where μ_r is the hole mobility, N_v is the effective density of states in the valance band, N_a and N_d are the concentrations of donors and acceptors, respectively, E_A is the ionization energy of the acceptor impurity responsible for the equilibrium conductivity of the semiconductor. Since $N_v \sim T^{3/2}$ and the hole mobility in CdTe μ_r is proportional to $T^{-3/2}$ within the temperature region $T > 200$ K [18, 19], one can consider that the temperature dependence of the serial resistance is mainly determined by the exponential factor, $R_s \sim \exp(-E_A/kT)$. Thereby the slope of the linear dependence $R_s(10^3/\mathrm{T})$ in the semilogarithmic coordinates determines the energy location of the working acceptor level $E_A = 0.3$ eV (the inset of figure 2).

The relatively large value of the serial resistance of the heterojunctions can be induced by an interfacial layer with a high resistance at the n-TiO_2/p-CdTe interface. The high-resistance layer can be formed due to the penetration of Ti atoms into the thin near-surface layer of p-CdTe substrates during TiO_2 thin films deposition. The average kinetic energy of magnetron-sputtered Ti atoms is equal to 8 eV (over 60 000 K) [20]; therefore, they can impact energetically on the near-surface layer of the CdTe substrates.

It is known that the elements with the unfilled 3d shell, including Ti, dissolve in the Cd sublattice and create deep energy levels in CdTe [21–24]. According to the work [24], the injection of Ti atoms into the CdTe lattice results in obtaining a high-resistance material, with the electric conductivity induced by the ionization of the deep energy level $E_c - (0.73 \pm 0.03)$ eV. In our case, this process leads to the compensation of shallow acceptor levels created by cadmium vacancies ($E_v + 0.05$ eV) resulting in the decrease of the conductivity of CdTe, which is finally determined by the ionization of acceptor levels located deeper in the band gap ($E_v + 0.3$ eV), as was shown above.

3.2. Current mechanisms

3.2.1. The forward bias. The energy-band diagram of an n-TiO_2/p-CdTe heterojucntion is very similar to that of a n-CdS/p-CdTe heterojunction [2, 8, 10, 25]. According to the analysis of the energy-band diagram [8] one can conclude that the main current mechanism for this kind of heterojunctions is generation-recombination processes within the depletion region via the deep levels located in the vicinity of the CdTe midgap. However, the conditions of the charge carrier's transport through the n-TiO_2/p-CdTe heterojunctions under consideration are complicated by the relatively high concentration of the surface states at the TiO_2/CdTe interface, which can play a role of the traps of charge carriers or recombination centers as well as participate in the multistep tunnel-recombination processes [26, 27].

Due to the small current flow through the heterojunctions at the low forward bias, the external voltage V is completely applied to the depletion region. Hence, there is no need to take into consideration the influence of the serial resistance R_s on the *I–V* characteristics of the heterojunctions.

Figure 3 shows the *I–V* characteristics of the n-TiO_2/p-CdTe heterojunctions at the low forward bias and different temperatures. The linear segments are seen within the forward bias $V > 3kT/e$ indicating the *I–V* exponential dependence.

It should be emphasized that the slope of the linear segments $\Delta\ln(I)/\Delta V$ does not depend on temperature ($3kT/e < V < 0.7$ V). This circumstance eliminates the

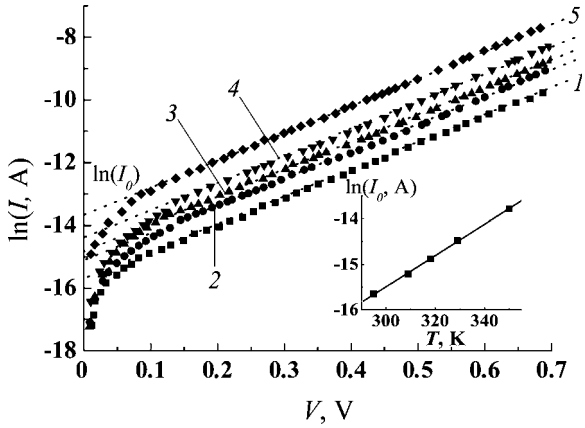

Figure 3. The *I–V* characteristics of the heterojunctions at the low forward bais in the semilogarithmic scale: 1—295 K, 2—309 K, 3—318 K, 4—329 K, 5—350 K. In the inset the temperature dependence of the cutoff current is shown.

possibility of analyzing the charge carrier's transport based on the generation-recombination processes within the depletion region because in this case a temperature dependence of the slope of the linear segments of *I–V* characteristics in the semilogarithmic coordinates must be observed $\Delta\ln(I)/\Delta V = e/nkT$, where n is the ideality coefficient [28]. The constant slope of the dependences ln(*I*)–*V* at different temperatures can be considered as the evidence of a tunnel nature of the dominating current mechanism [27, 29]. Since the linear segments of the *I–V* characteristics start at the low forward bias (figure 3), the space charge region is not thin enough for direct tunneling of charge carriers, which is described by the Newman formula [29]. Hence one can consider the multistep tunnel-recombination processes via the surface states at the TiO_2/CdTe interface to be the only physically based current mechanism. In this case, the current at the forward bias is governed by the following equation [29]:

$$I = B\exp(-\alpha(\varphi_0(T) - \mathrm{eV})) \tag{3}$$

$$\alpha \approx \frac{4}{3\hbar}\left(\frac{m_n^*\varepsilon_0\varepsilon_n}{N_D}\right)^{1/2}, \tag{4}$$

where B is the parameter which has small correlation with temperature and voltage, φ_0 is the height of the potential barrier, m_n^*, N_D, ε_n, are the electron effective mass, concentration of donors and relative permittivity of TiO_2, respectively.

Let us transform equation (3) into another form:

$$I = B\exp(-\alpha\varphi_0(T))\exp(\alpha\mathrm{eV}) = I_0\exp(\alpha\mathrm{eV}), \tag{5}$$

where $I_0 = B\exp(-\alpha\varphi_0(\mathrm{T}))$ is the cutoff current which is voltage independent. It is seen from equation (5) that the slope $\Delta\ln(I)/\Delta V$ of the linear segments of the *I–V* characteristics plotted in figure 3 determines the coefficient α, which is equal to 9.5 eV^{-1}.

Having taken into consideration the above-determined temperature dependence of the height of the potential barrier $\varphi_0(T)$, equation (1), the cutoff current I_0 can be calculated by equation (6):

$$\begin{aligned} I_0 &= B\exp(-\alpha(\varphi_0(0) - \beta_\varphi T)) \\ &= B\exp(-\alpha\varphi_0(0))\exp(\alpha\beta_\varphi T) = I_c\exp(\alpha\beta_\varphi T), \end{aligned} \tag{6}$$

where I_c is the constant.

The inset of figure 3 shows the temperature dependence $I_0(T)$ in the semilogarithmical coordinates. The coefficient α can be determined again from the slope of the linear dependence $\ln(I_0) - T$: $\alpha = \beta_\varphi{}^{-1}(\Delta\ln(I_c)/\Delta\mathrm{T}) = 10.8\ \mathrm{eV}^{-1}$. The coincidence of the values of the coefficient α, determined from the different dependences, equations (5) and (6), proves the validity of the analysis of the *I–V* characteristics of the n-TiO_2/p-CdTe heterojunctions at the low forward bias in the scope of the multistep tunnel-recombination model via the surface states at the TiO_2/CdTe interface.

The height of the potential barrier decreases as the forward bias increases. This process results in the appearance of the over barrier current. Within the applied voltage $V > 0.7$ V, the *I–V* characteristics are well described in terms of the emission-recombination mechanism taking into account the influence of the serial resistance R_s (the direct recombination of charge carriers via the energy levels at the interface, which is determined by the height of the potential barrier) [29]:

$$I = I_s\left[\exp\left(\frac{e(V - IR_s(T))}{AkT}\right) - 1\right], \tag{7}$$

where

$$I_s = B\exp\left(-\frac{\varphi_0(T)}{AkT}\right), \tag{8}$$

where B is the coefficient which is weakly dependent on temperature, the coefficient A, as usual, varies from 1 to 2. The experimental value $A = 1.9$ was determined from the dependences $\ln(I) = f(V–IR_s)$ at different temperatures.

In the case of the emission-recombination mechanism domination, the recombination centers are considered to be uniformly distributed over energy and localized in the vicinity of the interface.

Having found the logarithm of equation (7), we obtain

$$\ln(I) + \frac{eIR_s(T)}{AkT} = \ln(I_s) - \frac{\mathrm{eV}}{AkT}. \tag{9}$$

From the above equation it became evident that the dependences $\ln(I) + eIR_s(T)/AkT = f(V)$ have to be approximated by the straight lines with the temperature-dependent slope, that is seen in fact (figure 4).

The values of the cutoff current $\ln(I_s)$ were determined by the extrapolation of the linear segments toward interception with the current axis (figure 4). The energy slope of the linear dependence $\ln(I_s) = f(10^3/\mathrm{T})$ (the inset of figure 4) is equal to the height of the potential barrier at 0 K (equation (8)). The obtained value of $\varphi_0(0)$ is equal to 1.4 eV, that is, well correlated with the above-determined value $\varphi_0(0) = 1.47$ eV (the inset of figure 1).

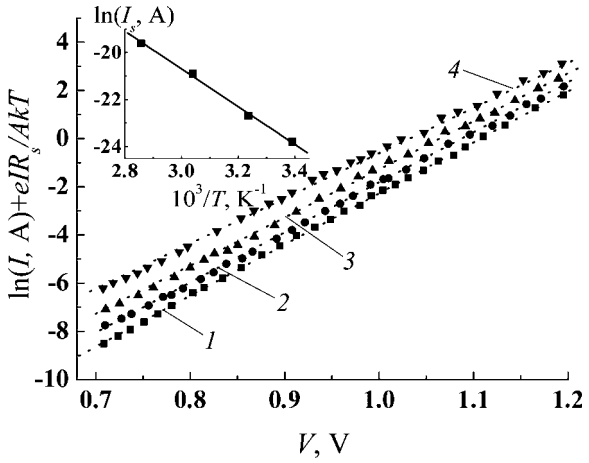

Figure 4. The *I–V* caracteristics of the heterojunctions at the forward bias $V > 0.7$ V: 1—295 K, 2—309 K, 3—329 K, 4—350 K. The inset shows the temperature dependence of the cutoff current I_s.

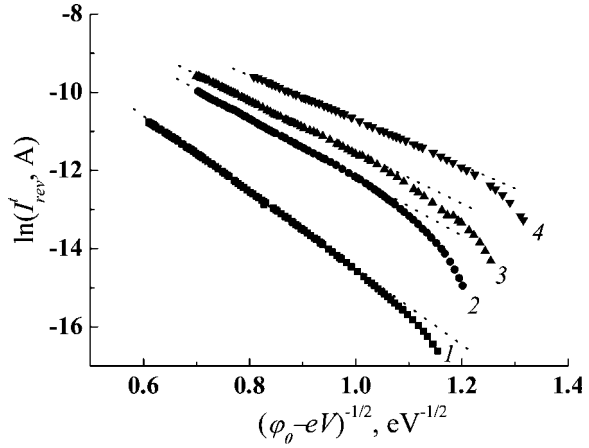

Figure 5. The tunnel mechanism of the current transport through the n-TiO_2/p-CdTe heterojunctions at the reverse bias: 1—295 K, 2—309 K, 3—329 K, 4—350 K.

3.2.2. The reverse bias. In the case of an abrupt heterojunction, the tunnel current at the reverse bias is governed by the following equation [29]:

$$I^t_{\rm rev} \approx a_0 \exp\left(-\frac{b_0}{\sqrt{\varphi_0(T) - {\rm eV}}}\right), \qquad (10)$$

where a_0 and b_0 are the voltage-independent parameters.

According to equation (10), the linear *I–V* characteristics in the coordinates $\ln(I^t_{\rm rev})$–$(\varphi_0–{\rm eV})^{-1/2}$ (figure 5) prove the domination of the tunnel mechanism of the charge carrier's transport at the reverse bias $|V| > 3kT/e$.

The slope of the linear segments decreases as temperature elevates (figure 5) due to the decrease of the parameter b_0, which is described by the following equation [28]:

$$b_0 = C W_1(T) \varphi_0(T)^{3/2}, \qquad (11)$$

where C constant, W_1 is the width of the space charge region at $\varphi_0 - {\rm eV} = 1$ eV. The width of the space charge region of an abrupt asymmetrical heterojunction can be calculated from the following equation [30]:

$$W = \sqrt{\frac{2\varepsilon_0 \varepsilon_p (\varphi_0 - {\rm eV})}{e\,(N_A - N_D)}}, \qquad (12)$$

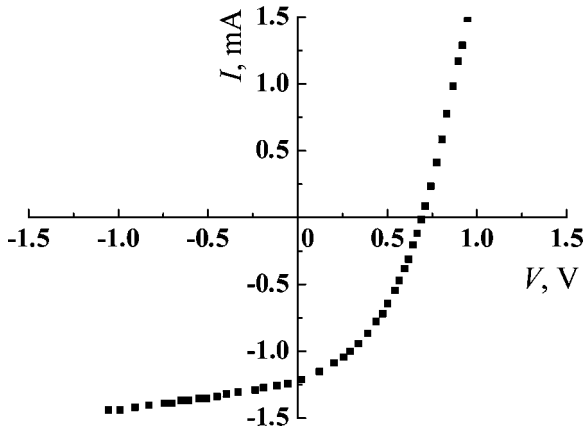

Figure 6. The light *I–V* characteristic of the n-TiO_2/p-CdTe heterojunctions for 100 mW cm^{-2} illumination.

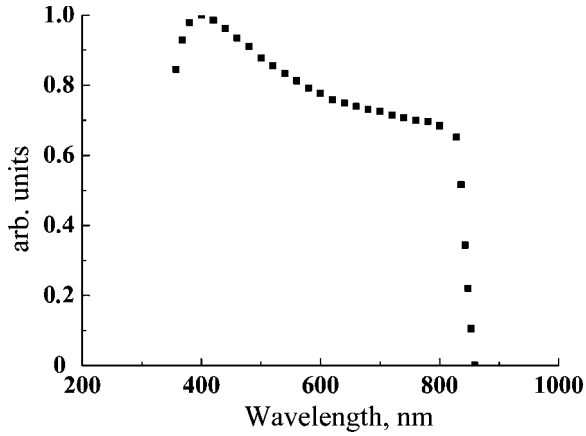

Figure 7. The spectral distribution of the external quantum efficiency of the n-TiO_2/p-CdTe heterojunctions.

where ε_0 is the absolute permittivity, ε_r is the relative permittivity of CdTe, $N_A - N_D$ gives the concentration of the uncompensated acceptors.

The parameter a_0 is determined by the occupation probability of the level from which the tunneling takes place at the reverse bias. Its energy location can be determined from the slope of the temperature dependence $\ln(a_0) = f(10^3/T)$ [28, 31]. However, the experimental data provide evidence that the parameter a_0 is temperature independent. It is typical for a metal–semiconductor contact under tunneling via metal's levels [31]. The temperature independence of the parameter a_0 can be a result of the participation of the surface states with the uniform energy distribution in tunneling processes.

3.3. Photoelectrical properties

The light *I–V* characteristic of the n-TiO_2/p-CdTe heterojunctions shows that they produce the open-circuit voltage $V_{\rm oc} = 0.69$ V, the short-circuit current $I_{\rm sc} = 6$ mA cm^{-2} and the fill factor FF = 0.43 under illumination of 100 mW cm^{-2} (figure 6).

The spectral distribution of the external quantum efficiency $\eta(\lambda)$ of the n-TiO_2/p-CdTe heterojunctions,

determined as the ratio of the short circuit current to the number of incident photons under illumination from the TiO_2 side is shown in figure 7. The location of the long-wave edge of the spectral distribution of the external quantum yield is well correlated with the band gap energy of CdTe. The short-wave edge of the spectrum is not measured entirely due to the ultraviolet limit of the halogen quartz lamp used in our spectrophotometer. In spite of this, figure 7 shows that the spectral region of the photosensitivity of a TiO_2/CdTe heterojunction is wider than that of a CdS/CdTe heterojunction [4, 7], as assumed above.

4. Conclusion

The temperature dependences of the height of the potential barrier and the serial resistance of the n-TiO_2/p-CdTe heterojunctions were investigated. The reason for the relatively large serial resistance was discussed.

It was established that the mechanisms of the current transport through the n-TiO_2/p-CdTe heterojunctions at the forward biases are well described in the scope of the multistep tunnel-recombination and emission-recombination models. The main mechanism of the charge carrier's transport through the heterojunctions at the reverse bias is the tunneling through the space charge region via the energy levels created by surface states.

From the above-mentioned fact, it becomes evident that the dominating mechanisms of the current transport through the heterojunctions are determined by the influence of the surface states at the TiO_2/CdTe interface.

The large concentration of the surface states at the interface of the heterojunctions under consideration and their relatively high serial resistance strongly influence the conditions of the current transport and photoelectric conversion in the n-TiO_2/p-CdTe heterojunctions. As a result, they produce the relatively low photoelectrical parameters: the short circuit current $I_{sc} = 6$ mA cm^{-2} and the fill factor FF $= 0.42$ under 100 mW cm^{-2} illumination.

At the same time a TiO_2 thin film, as a window layer, increases the width of the photosensitivity region of solar cells based on CdTe, in particular CdS/CdTe, thereby enhances their operational characteristics.

It is worth noting that the heterojunctions under consideration were fabricated without the optimization of technological parameters and additional treatments. It is obvious that the controllable change of technological parameters of the TiO_2 thin films' deposition, modification of the CdTe surface, annealing of the heterojunctions in different environments as well as the introduction of additional intermediate layers can reduce the surface states' concentration at the TiO_2/CdTe interface and enhance the efficiency of the photoelectric conversion.

One of the approaches to enhance the photoelectric conversion in the n-TiO_2/p-CdTe heterojunctions, mentioned above, is going to become the subject of our investigation in the near future.

References

[1] Alferov Zh I 1998 *Fiz. Tekh. Poluprovodn.* **32** 3
[2] Soga T 2006 *Nanostructured Materials for Solar Energy Convertion* (Amsterdam: Elsevier) p 615
[3] Pantoja Enriquez J, Methew X, Hernandez G P, Pal U, Magana C, Acosta D R, Guardian R, Toledo J A, Contreras Puente G and Chavez Carvayar J A 2004 *Sol. Energy Mater. Sol. Cells* **82** 307
[4] Kosyachenko L, Lasharev G, Grushko E, Ievtushenko A, Sklyarchuk V, Methew X and Paulson P D 2009 *Acta Phys. Pol.* A **116** 862
[5] Khrypunov G S, Chernyk E P, Kovtun N A and Belonogov E K 2009 *Semiconductors* **43** 1046
[6] National Renewable Energy Laboratory 2001 <www.nrel.gov/news/press/2001/1501_record.html>
[7] Kosyachenko L A 2006 *Semiconductors* **40** 710
[8] Kosyachenko L A, Mathew X, Motushchuk V V and Sclyarchuk V M 2005 *Semiconductors* **39** 539
[9] Kosyachenko L A and Grushko E V 2010 *Semiconductors* **44** 1375
[10] Kosyachenko L 2010 Efficiency of thin-film CdS/CdTe solar cells *Solar Energy* ed R D Rugescu (Croatia: INTECH) pp 105–30
[11] Diebold U 2003 *Surf. Sci. Rep.* **43** 53
[12] Richards B S 2002 Novel uses of titanium dioxide for silicon solar cells *PhD Thesis*, University of New South Wales, Sydney
[13] Brus V V 2010 *Eastern-Eur. J. Enterprise Technol.* **47** 13
[14] Ernst K, Engelhardt R, Ellmer K, Kelch C, Muffler H J, Lux-Steiner M Ch and Konenkamp R 2001 *Thin Solid Films* **387** 26
[15] Ernst K, Belaidi A and Konenkamp R 2003 *Semicond. Sci. Technol.* **18** 475
[16] Brus V V, Kovalyuk Z D, Marianchuk P D, Orletsky I G and Maystruk E V 2010 *TKEA* **89** 60
[17] Kosyachenko L A, Methew X, Motushchuk V V and Sklyarchuk V M 2006 *Sol. Energy* **80** 148
[18] Aven M and Prener J S 1967 *Physics and Chemistry of II–VI Compounds* (Amsterdam: North-Holland)
[19] Kosyachenko L A, Sklyarchuk V M, Sklyarchuk Ye F and Ulyanitsky K S 1999 *Semicond. Sci. Technol.* **14** 373
[20] Milton Ohring 1992 *The Materials Science of Thin Films* (San Diego, CA: Academic) 704
[21] Kikoin K A, Kurik I G and Melnichuk S V 1990 *Fiz. Tekh. Poluprovodn.* **24** 587
[22] Hofmann D M, Stadler W, Christmann P and Meyer B K 1996 *Nucl. Instrum. Methods Phys. Res.* A **380** 117
[23] Rzepka E, Marfaing Y, Cuniot M and Triboulet R 1993 *Mater. Sci. Eng.* B **16** 262
[24] Babiy P I, Slyn'ko B B, Gnatenko Yu P, Ilashchuk M I and Parfenyuk O A 1990 *Fiz. Tek. Poluprovodn.* **24** 1444
[25] Brus V V, Ilashchuk M I, Kovalyuk Z D, Maryanchuk P D, Ulyanytsky K S and Gritsyuk B N 2011 *Semiconductors* **45** 1077
[26] Makhniy V P, Khusnutdinov S V and Gorley V V 2009 *Acta Phys. Pol.* A **116** 859
[27] Fahrenbruch A L and Bube R H 1983 *Fundamentals of Solar Cells. Photovoltaic Solar Energy Conversion* (New York: Academic) 236
[28] Gorley P M, Grushka Z M, Makhniy V P, Grushka O G, Chervinsky O A, Horley P P, Vorobiev Yu V and Gonzalez-Hernandez J 2008 *Phys. Status Solidi* C **5** 3622
[29] Sharma B L and Purohit R K 1974 *Semiconductor Heterojunctions* (New York: Pergamon) 216
[30] Sze S M and Kwok K 2007 *Physics of Semiconductor Devices* 3rd edn (New Jersey: Wiley) 815
[31] Machniy V P and Skrypnyk N J 2011 *Semiconductors* **43** 312